RESEARCH ARTICLE

Modeling of [18F]FEOBV Pharmacokinetics in Rat Brain

Anna Schildt,[1,2] Erik F.J. de Vries,[1] Antoon T.M. Willemsen,[1] Rodrigo Moraga-Amaro,[1] Bruno Lima-Giacobbo,[1] Jürgen W.A. Sijbesma,[1] Vesna Sossi,[2] Rudi A.J.O. Dierckx,[1] Janine Doorduin ⓘ[1]

[1]Department of Nuclear Medicine and Molecular Imaging, University of Groningen, University Medical Center Groningen, P.O Box 30.001, Groningen, 9700RB, The Netherlands
[2]Department of Physics and Astronomy, University of British Columbia, Vancouver, Canada

Abstract

Purpose: [18F]Fluoroethoxybenzovesamicol ([18F]FEOBV) is a radioligand for the vesicular acetylcholine transporter (VAChT), a marker of the cholinergic system. We evaluated the quantification of [18F]FEOBV in rats in control conditions and after partial saturation of VAChT using plasma and reference tissue input models and test-retest reliability.

Procedure: Ninety-minute dynamic [18F]FEOBV PET scans with arterial blood sampling were performed in control rats and rats pretreated with 10 μg/kg FEOBV. Kinetic analyses were performed using one- (1TCM) and two-tissue compartmental models (2TCM), Logan and Patlak graphical analyses with metabolite-corrected plasma input, reference tissue Patlak with cerebellum as reference tissue, standard uptake value (SUV) and SUV ratio (SUVR) using 60- or 90-min acquisition. To assess test-retest reliability, two dynamic [18F]FEOBV scans were performed 1 week apart.

Results: The 1TCM did not fit the data. Time-activity curves were more reliably estimated by the irreversible than the reversible 2TCM for 60 and 90 min as the influx rate K_i showed a lower coefficient of variation (COV, 14–24 %) than the volume of distribution V_T (16–108 %). Patlak graphical analysis showed a good fit to the data for both acquisition times with a COV (12–27 %) comparable to the irreversible 2TCM. For 60 min, Logan analysis performed comparably to both irreversible models (COV 14–32 %) but showed lower sensitivity to VAChT saturation. Partial saturation of VAChT did not affect model selection when using plasma input. However, poor correlations were found between irreversible 2TCM and SUV and SUVR in partially saturated VAChT states. Test-retest reliability and intraclass correlation for SUV were good.

Conclusion: [18F]FEOBV is best modeled using the irreversible 2TCM or Patlak graphical analysis. SUV should only be used if blood sampling is not possible.

Key Words: Animal studies, Cognition, Neurotransmitters, Kinetic modeling, Positron emission tomography

Introduction

The decline of cognitive function in neurological disorders, such as Alzheimer's disease (AD) [1], Parkinson's disease (PD), and PD with dementia [2, 3], has been associated with degeneration of cholinergic neurons. To study the role of

changes in cholinergic innervation, *ex vivo* tissue analysis is widely used. Nevertheless, the use of the non-invasive imaging technique positron emission tomography (PET) imaging is often the preferred method, as it allows the assessment of neurotransmitter systems *in vivo*.

[18F]fluoroethoxybenzovesamicol ([18F]FEOBV) is a PET radioligand with high specificity for the presynaptic vesicular acetylcholine transporter (VAChT). The expression of VAChT was found to correlate well with the expression of the main marker of cholinergic neurons, choline acetyltransferase [4]. In rats and non-human primates, [18F]FEOBV distribution in the brain was found to correlate with VAChT expression, with the highest uptake in the striatum and lowest in the cerebellum [5, 6].

Pharmacokinetic modeling with arterial plasma input is the gold standard to quantify the binding of a radioligand to its target. Kinetic analysis of [18F]FEOBV in humans showed that the kinetic model parameters could be reliably estimated using metabolite-corrected plasma input and long scan times (360 min) [7]. Quantification using reference tissue modeling with shorter scan times, or late static scanning, was found to correlate well with the results from pharmacokinetic modeling with arterial plasma input. These simplified methods are preferred over the use of plasma input models as arterial sampling is a complex procedure and a burden for human subjects.

While quantification of [18F]FEOBV has been evaluated in humans, quantification of [18F]FEOBV in rats has only been performed using reference tissue models [8] without validation of their use against compartmental models using arterial plasma input. Examples of other radiotracers, such as [11C]flumazenil, have shown that interspecies differences between humans and rats can lead to different preferred compartmental models for each species [9]. Therefore, the purpose of this study was to determine the optimal quantification model for [18F]FEOBV using a plasma input function and to verify quantification without the need for blood sampling.

Materials and Methods

Experimental Animals

Adult male Wistar rats (364 ± 39 g, Envigo, The Netherlands) were randomly divided in three groups, *i.e.*, control ($n = 6$), pretreatment with FEOBV ($n = 6$), and test-retest ($n = 6$). Rats were group-housed at a 12 h/12 h light/dark cycle, in humidity- and temperature-controlled (21 ± 2 °C) rooms with water and standard laboratory chow available *ad libitum* and acclimatized for at least 7 days after arrival. All experiments were approved by the National Committee on Animal Experiments (CCD:AVD105002015166) and the Institutional Animal Care and Use Committee of the University of Groningen (IvD:15166-01-003). All applicable institutional and/or national guidelines for the care and use of animals were followed.

PET Imaging

The rats were anesthetized with isoflurane (5 % for induction, 1–2.5 % for maintenance) mixed with oxygen. A cannula was placed in the tail vein for [18F]FEOBV injection. For the control and pretreatment group, a cannula was placed in the femoral artery for arterial blood sampling. Rats were injected i.p. with 100 µl DMSO 50–80 min before [18F]FEOBV injection (controls) or with 10 µg/kg FEOBV (pretreatment, ABX, Germany) in 200 µl DMSO *via* the femoral vein 20–30 min before injection. It is not expected that the administration route of DMSO affects the binding of [18F]FEOBV [10]. Rats were then placed in a small animal PET scanner (Focus 220, Siemens Healthcare, USA) with their head in the center of the field of view. A transmission scan with a Co-57 point source was performed first. The rats were then injected with 28.3 ± 7.3 MBq [18F]FEOBV (molecular activity > 150TBq/mmol, injected dose 0.03 ± 0.01 µg) over 1 min using an infusion pump (1 ml/min), and a 90-min dynamic PET scan was started. Rats in the test-retest group were not subjected to arterial blood sampling and underwent a second PET scan 7 days later. During all procedures, eye salve was applied to prevent dehydration of the eyes, body temperature was maintained and oxygen saturation and heart rate were monitored. [18F]FEOBV was synthesized according to the procedure described by Mulholland et al. [11].

Arterial Blood Sampling and Metabolite Analysis

Blood samples (0.10–0.13 ml) were taken from the femoral artery at 10, 20, 30, 40, and 50 s and 1, 1.5, 2, 3, 5, 7.5, 10, 15, 30, 60, and 90 min after [18F]FEOBV injection. Plasma was obtained by centrifugation of whole blood (5 min at 30,000×g). After collection of each blood sample, the same volume of heparinized saline was injected to compensate for the blood volume loss. The radioactivity in 25 µl of whole blood and 25 µl of plasma was measured with an automated well-counter (Wizard2480, PerkinElmer, USA) and decay corrected.

All plasma samples were used for metabolite analysis. After adding 50 µl acetonitrile, each sample was vortexed and centrifuged (8 min at 3000×g). Supernatant (1–2 µl) was pipetted onto a silica gel 60 F_{254} plate (Merck, Germany) and eluted with a mixture of hexane/dichlormethane/diethyl-ether/triethylamine (2.3/1/1/0.2). A phosphor storage screen (PerkinElmer, USA) was exposed to the silica plates overnight and scanned with a Cyclone (PerkinElmer, USA). The percentage of intact tracer was assessed using OptiQuant Software 3.

Pharmacokinetic Analysis

Listmode data were iteratively reconstructed into 24 frames (6 × 10, 4 × 30, 2 × 60, 1 × 120, 1 × 180, 4 × 300, 6 × 600 s)

using OSEM2D after Fourier Rebinning (4 iterations, 16 subsets), and normalized and corrected for attenuation, scatter, and decay.

PMOD 3.9 software was used for registration of each PET image to a tracer-specific template [12] and for pharmacokinetic modeling. A volume of interest (VOI) template (including frontal cortex, remainder of the cortex (referred to as cortex), striatum, thalamus, hypothalamus, hippocampus, and cerebellum) was placed on the co-registered individual PET images and manually adjusted as a group, if necessary. Time-activity curves for each VOI were generated for 60-min and 90-min acquisition lengths.

For pharmacokinetic analysis, arterial input-based models were evaluated first. One- (1TCM) and two-tissue compartmental models (2TCM) were evaluated, using metabolite-corrected plasma and whole blood input. Two rate constants (K_1, k_2) were determined for the 1TCM and four (K_1-k_4, reversible) or three rate constants (K_1-k_3, irreversible) for the 2TCM. The volume of distribution, V_T, was calculated for the reversible ($V_T = (K_1/k_2)(1 + k_3/k_4)$) and the influx rate K_i for the irreversible ($K_i = (K_1 * k_3)/(k_2 + k_3)$) 2TCM. Logan and Patlak graphical analyses were performed with a t* of 25 and 10 min, respectively [13, 14]. The blood volume fraction in tissue was fixed at 5 %. Akaike information criterion (AIC) and the coefficient of variation (COV) of the outcome parameters were used to select the best model. The COV was calculated as standard deviation (SD) divided by the mean.

Second, K_i^{ref} was estimated using reference Patlak (t* of 10 min) with the cerebellum as reference tissue [15].

Third, the standardized uptake value (SUV) was calculated ((radioactivity concentration in VOI)/(injected radioactivity/body weight)) for the periods of 50–90 min and 30–60 min. The standardized uptake value ratio (SUVR) was obtained by dividing the target SUV by the reference tissue (cerebellum) SUV.

For the test-retest scans, only the most promising simplified measure (SUV) was used. The test-retest variability was calculated as (2x|test–retest|/(test+retest)) × 100% for SUV. The interclass correlation coefficient (ICC) was calculated as an index of the reliability of the test-retest measurement using all brain regions, ICC ≥ 0.75 representing good agreement [15].

Statistical Analysis

All data are presented as mean ± SD. Statistical analysis was performed using SPSS24. Linear regression was used to determine the correlation between the different outcome measures. To assess the sensitivity of the outcome measures, the differences between groups (control and pretreatment with FEOBV) were evaluated using a two-way ANOVA with "brain region," "group" as main effects, and "brain region × group" as the interaction effect, with Bonferroni *post hoc* testing. Additionally, receiver operator curves

(ROC) and their area under the curve (AUC) were used to evaluate the ability of outcome measures to differentiate between the two groups. AUC values range from 0.5 to 1, with 1 representing perfect and 0.5 no separation between groups [16]. For test-retest scans, a repeated-measures ANOVA with "time," "brain region" as main effects, and "time × brain region" as interaction effect, was performed.

Results

Two rats were excluded from the final analysis. One control rat was considered an outlier as the macroparameters from multiple kinetic models were > 1.5 times the interquartile range, and one rat pretreated with FEOBV showed displacement by the pretreatment only 60 min after [^{18}F]-FEOBV injection. Four rats (2 control and 2 pretreated with FEOBV) had incomplete blood, plasma, or metabolite curves; missing data points were estimated by fitting a population-based curve to available points.

Tracer Kinetics and Metabolism

All brain regions showed rapid accumulation of [^{18}F]FEOBV and a VAChT expression-dependent distribution, with highest uptake in striatum (high VAChT expression) and lowest in cerebellum (low VAChT expression). In striatum, 25 ± 11 % of initial [^{18}F]FEOBV uptake was cleared at 60 min, while 60 ± 3 % was cleared from cerebellum (Fig. 1). Both regions showed almost no clearance of [^{18}F]FEOBV between 60 and 90 min. Pretreatment with FEOBV resulted in a similar distribution pattern and time-activity curve as controls, although [^{18}F]FEOBV uptake was reduced compared to controls by 10 % and 2 % at 90 min in the striatum and cerebellum, respectively.

In blood and plasma, [^{18}F]FEOBV uptake was highest at 1 min, followed by a rapid clearance with only 22 ± 4 % of radioactivity remaining in plasma and 26 ± 3 % in blood at 3 min after injection (Fig. 1). After 90 min, 17 ± 5 and 20 ± 3 % of radioactivity remained in plasma and blood, respectively. Similar kinetic behavior in plasma and blood was found in the FEOBV pretreatment group. [^{18}F]FEOBV was metabolized rapidly in plasma with 46 ± 4 % remaining intact at 3 min and 2 ± 0.2 % at 90 min. After pretreatment with FEOBV, 55 ± 5 % and 4 ± 2 % of intact tracer remained at 3 and 90 min, respectively.

Plasma Input Models

Compartmental Models   The 1TCM did not fit the data. The reversible and irreversible 2TCM showed good fits for 60 and 90 min (Suppl. Fig. 1, see Electronic Supplementary Material (ESM)). The AIC of the reversible and the irreversible 2TCM were similar, but 13–18 % lower for 60 than 90 min (Table 1).
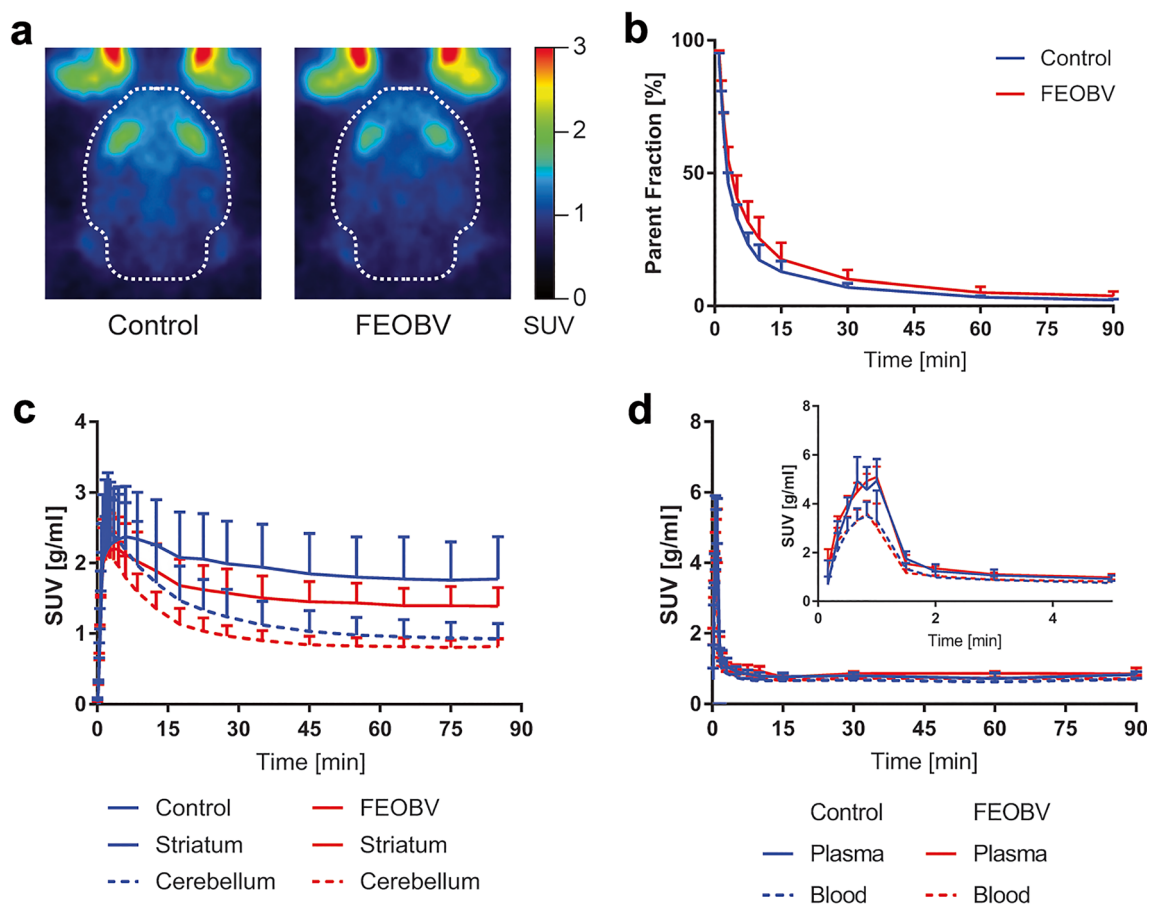
Fig. 1 Kinetic behavior of [¹⁸F]FEOBV in control rats and rats pretreated with 10 µg/kg FEOBV. **a** Average SUV images of control and pretreated rats (brain outline: dashed line). **b** Fraction of intact [¹⁸F]FEOBV over time. Time course of [¹⁸F]FEOBV uptake in **c** striatum and cerebellum and **d** plasma and blood. Data are shown as mean ± standard deviation.

The 60 min V_T values from the reversible 2TCM for different brain regions ranged from 11 to 65 ml/cm³ for the control group, and from 6 to 30 ml/cm³ for the group pretreated with FEOBV (Table 1). The COV was higher for the control group (16–77 %) than for the pretreated group (21–34 %). The V_T values obtained with 90 min were higher than those with 60 min with a higher COV, *i.e.*, 16 to 120 ml/cm³ (COV 16–108 %) for the control and 10 to 68 ml/cm³ (COV 29–80 %) for the pretreated group. Linear regression showed a poor correlation between V_T from 60 and 90 min for controls ($R^2 = 0.15$, $V_T(90\ \mathrm{min}) = 14.2 + 1.0 \times V_T(60\ \mathrm{min})$, $p = 0.01$) and a moderate correlation for the pretreated group ($R^2 = 0.45$, $V_T(90\ \mathrm{min}) = 0.5 + 1.7 \times V_T(60\ \mathrm{min})$, $p < 0.0001$). For the control and the pretreatment group, the rate constants K_1 and k_2 showed lower variability (K_1, COV 14–36 %, k_2, COV 10–48 %) than the rate constants k_3 and k_4 (k_3, COV 11–81 %, k_4, COV 17–71 %) for 60 and 90 min. In the control group, the average rate constants in the striatum were 0.48 ± 0.08 ml/cm³/min for K_1, 0.089 ± 0.02 min⁻¹ for k_2, 0.0698 ± 0.031 min⁻¹ for k_3 and 0.0146 ± 0.004 min⁻¹ for k_4 with 60-min acquisition time, while they were 0.45 ± 0.1 ml/cm³/

min for K_1, 0.129 ± 0.03 min⁻¹ for k_2, 0.0579 ± 0.016 min⁻¹ for k_3, and 0.0132 ± 0.006 min⁻¹ for k_4 in the FEOBV pretreatment group.

The irreversible 2TCM with 60 min estimated K_i values of 0.065–0.209 ml/cm³/min for the control group and 0.042–0.128 ml/cm³/min for the group pretreated with FEOBV. Similar values were found for 90 min (control, 0.060–0.193 ml/cm³/min; pretreated, 0.038–0.116 ml/cm³/min). The K_i showed less variation than V_T, with a COV of 14–24 % for the control and pretreated groups, for both 60 and 90 min. Linear regression revealed a good correlation between 60 and 90 min with an R^2 of 0.97 ($K_i(90\ \mathrm{min}) = 0.9 \times K_i(60\ \mathrm{min})$, $p < 0.0001$) for control and R^2 of 0.90 ($K_i(90\ \mathrm{min}) = 0.006 + 0.8 \times K_i(60\ \mathrm{min})$, $p < 0.0001$) for pretreated group. The rate constants K_1, k_2, and k_3 derived from the irreversible 2TCM showed a lower variation compared to the reversible 2TCM with COV ranging between 5 and 38 % in the control and 10 and 37 % in the pretreated group. In the striatum with 60-min acquisition time, average values of 0.44 ± 0.08 ml/cm³/min for K_1, 0.059 ± 0.02 min⁻¹ for k_2, and 0.0304 ± 0.005 min⁻¹ for k_3 were estimated in the control group. In the pretreatment

Table 1. V_T and K_i estimated by 2TCM and graphical analysis for 60 and 90 min. Significant differences between control and pretreatment group are indicated as ***$p < 0.0005$, **$p < 0.005$, *$p < 0.05$. Shown are mean ± standard deviation ($n = 5$) for macroparameter and AIC and the range of the COV

Brain region	Reversible 2TCM [V_T]		Irreversible 2TCM [K_i]		Logan [V_T]		Patlak [K_i]	
	Control	FEOBV	Control	FEOBV	Control	FEOBV	Control	FEOBV
60 min								
Brainstem	16.9 ± 2.7	10.7 ± 2.3	0.112 ± 0.019	0.074 ± 0.012**	16.2 ± 3.3	10.5 ± 2.2*	0.086 ± 0.012	0.051 ± 0.011***
Cerebellum	14.2 ± 4.6	9.7 ± 3.3	0.081 ± 0.012	0.058 ± 0.012*	11.7 ± 2.2	8.5 ± 1.7	0.059 ± 0.008	0.041 ± 0.011*
Cortex	17.1 ± 5.5	11.7 ± 3.2	0.091 ± 0.013	0.068 ± 0.010*	13.6 ± 2.6	9.8 ± 1.5	0.077 ± 0.009	0.05 ± 0.009**
Frontal cortex	27.6 ± 21.3	13.9 ± 3.8**	0.116 ± 0.016	0.086 ± 0.009*	17.7 ± 3.6	12.5 ± 1.7*	0.101 ± 0.012	0.065 ± 0.009***
Hippocampus	16.8 ± 2.9	11.8 ± 3.7	0.097 ± 0.015	0.072 ± 0.012*	14.3 ± 2.5	10.3 ± 1.6*	0.078 ± 0.010	0.051 ± 0.01**
Hypothalamus	21.1 ± 3.3	13.3 ± 3.9	0.119 ± 0.020	0.081 ± 0.015**	17.3 ± 3.4	11.8 ± 2.2*	0.097 ± 0.013	0.059 ± 0.014***
Striatum	30.8 ± 7.8	20.6 ± 6.3*	0.152 ± 0.037	0.103 ± 0.016***	24.8 ± 8	15.7 ± 2.8***	0.133 ± 0.032	0.082 ± 0.013***
Thalamus	17.8 ± 3.4	11.6 ± 2.6	0.108 ± 0.018	0.080 ± 0.015*	15.9 ± 2.9	11.2 ± 1.6*	0.086 ± 0.012	0.053 ± 0.012***
COV	16–77 %	21–34 %	14–24 %	15–21 %	18–32 %	14–21 %	12–24 %	14–27 %
AIC	299 ± 19	283 ± 36	306 ± 15	297 ± 39	49 ± 4	49 ± 4	− 2 ± 7	− 7 ± 7
90 min								
Brainstem	26.4 ± 4.2	20.1 ± 10.1	0.103 ± 0.017	0.066 ± 0.01***	25.2 ± 5.1	13.2 ± 3**	0.084 ± 0.012	0.054 ± 0.01***
Cerebellum	37.6 ± 40.5	22.6 ± 17.1	0.076 ± 0.011	0.054 ± 0.01*	23.5 ± 11.6	11.2 ± 2.7**	0.062 ± 0.009	0.045 ± 0.008*
Cortex	44.0 ± 40.4	28.3 ± 22.6	0.086 ± 0.014	0.062 ± 0.009*	22.5 ± 5.8	12.6 ± 2.2*	0.074 ± 0.010	0.052 ± 0.007*
Frontal cortex	28.4 ± 8.6	22.6 ± 8.3	0.103 ± 0.015	0.077 ± 0.008*	23.8 ± 4.5	15.3 ± 2.3*	0.089 ± 0.012	0.064 ± 0.008**
Hippocampus	29.1 ± 15.4	17.4 ± 5.3	0.088 ± 0.015	0.063 ± 0.009*	21.5 ± 5.9	12.5 ± 2.1*	0.074 ± 0.011	0.051 ± 0.007*
Hypothalamus	32.8 ± 9.8	22.4 ± 10.4	0.107 ± 0.015	0.072 ± 0.012**	26.1 ± 4.0	14.7 ± 3.2**	0.090 ± 0.011	0.059 ± 0.011***
Striatum	53.6 ± 39.8	31.2 ± 9.6	0.143 ± 0.035	0.094 ± 0.014***	43.1 ± 15.0	19.9 ± 3.6***	0.129 ± 0.032	0.081 ± 0.010***
Thalamus	24.8 ± 5.5	17.1 ± 4.9	0.097 ± 0.017	0.068 ± 0.011**	22.5 ± 4.3	13.3 ± 2.1*	0.079 ± 0.012	0.053 ± 0.008**
COV	16–108 %	29–80 %	14–24 %	14–19 %	19–49 %	15–23 %	12–25 %	12–19 %
AIC	347 ± 24	349 ± 16	352 ± 18	362 ± 17	83 ± 4	82 ± 4	5 ± 9	− 6 ± 8

V_T in ml/cm^3, K_i in ml/cm^3/min
COV coefficient of variation, *AIC* Akaike information criterion

group, K_1 was $0.42 ± 0.01$ ml/cm^3/min, k_2 $0.096 ± 0.02$ min^{-1}, and k_3 was estimated as $0.0319 ± 0.008$ min^{-1} in the striatum.

Graphical Analysis Logan and Patlak graphical analysis showed a good fit of the data, with AIC values similar for the control and pretreated groups, but lower for 60 than 90 min. The V_T values from Logan graphical analysis (Table 1) for 60 min were 9–37 ml/cm^3 (COV 18–32 %) for the control group and 6–19 ml/cm^3 (COV 14–21 %) for the pretreated group. Higher V_T values were found for 90 min, *i.e.*, 12–47 ml/cm^3 (COV 19–49 %) for the control and 7–24 ml/cm^3 (COV 15–23 %) for the pretreated group. The V_T values from Logan analysis for the two acquisition lengths correlated well (control, $R^2 = 0.73$, $V_T(90 \text{ min}) = − 1 + 1.6 \times V_T(60 \text{ min})$, $p < 0.0001$; pretreated, $R^2 = 0.94$, $V_T(90 \text{ min}) = − 0.05 + 1.3 \times V_T(60 \text{ min})$, $p < 0.0001$). The correlation between V_T from Logan and the reversible 2TCM was moderate to poor ($R^2 = 0.29$–0.56, slope = 0.2–0.4, $p < 0.0001$).

Patlak graphical analysis of 60 min data resulted in K_i values of 0.053–0.184 ml/cm^3/min (COV 12–24 %) for controls and of 0.023–0.098 ml/cm^3/min (COV 14–27 %) after pretreatment. Similar values and a similar COV were found for 90 min (control, 0.051–0.175 ml/cm^3/min; pretreated, 0.032–0.092 ml/cm^3/min). Linear regression of K_i between 60 and 90 min showed good correlations for the control ($R^2 = 0.93$, $K_i(90 \text{ min}) = 0.004 + 0.9 \times K_i(60 \text{ min})$, $p < 0.001$) and pretreated group ($R^2 = 0.89$, $K_i(90 \text{ min}) = 0.01 + 0.8 \times K_i(60 \text{ min})$, $p < 0.001$). The K_i from Patlak correlated well with the K_i from the irreversible 2TCM with good R^2 for 60 min (control, $R^2 = 0.86$, $K_i(\text{Patlak}) = − 0.002 + 0.8 \times K_i(2TCM)$; pretreated, $R^2 = 0.89$, $K_i(\text{Patlak}) = − 0.01 + 0.9 \times K_i(2TCM)$) and 90 min (control, $R^2 = 0.95$, $K_i(\text{Patlak}) = − 0.003 + 0.9 \times K_i(2TCM)$; pretreated, $R^2 = 0.87$, $K_i(\text{Patlak}) = 0.8 \times K_i(2TCM)$) ($p < 0.001$).

Sensitivity of Plasma Input Models to VAChT Saturation Pretreatment with FEOBV resulted in a (statistically significant) decrease in V_T (20–54 %) and K_i (25–42 %), in all brain regions. The reversible 2TCM revealed a statistically significant decrease in V_T in the striatum (33 %, $p = 0.02$) and frontal cortex (50 %, $p = 0.002$) for 60 min but not for 90 min. Statistically significant decreases in K_i from the irreversible 2TCM were found in all brain regions for 60 and 90 min ($p < 0.05$). K_i was decreased by $30 ± 4$ % on average, with the largest decrease in the brainstem (60 min, 34 %; 90 min, 36 %) and the smallest decrease in the cortex (60 min, 25 %) and frontal cortex (90 min, 25 %).

Logan analysis with 90 min acquisition revealed a statistically significant decrease in V_T for all brain regions (45 %, $p < 0.05$), with the largest decrease in the striatum (54 %) and the smallest in the frontal cortex (36 %). For 60 min, a significant decrease in V_T was found in the brainstem, frontal cortex, hippocampus, hypothalamus, striatum, and thalamus (28–35 %, $p < 0.05$). Patlak analysis with 60 min showed a statistically significant decrease in K_i for all brain regions ($37 ± 3$ %; $p < 0.05$), with the largest
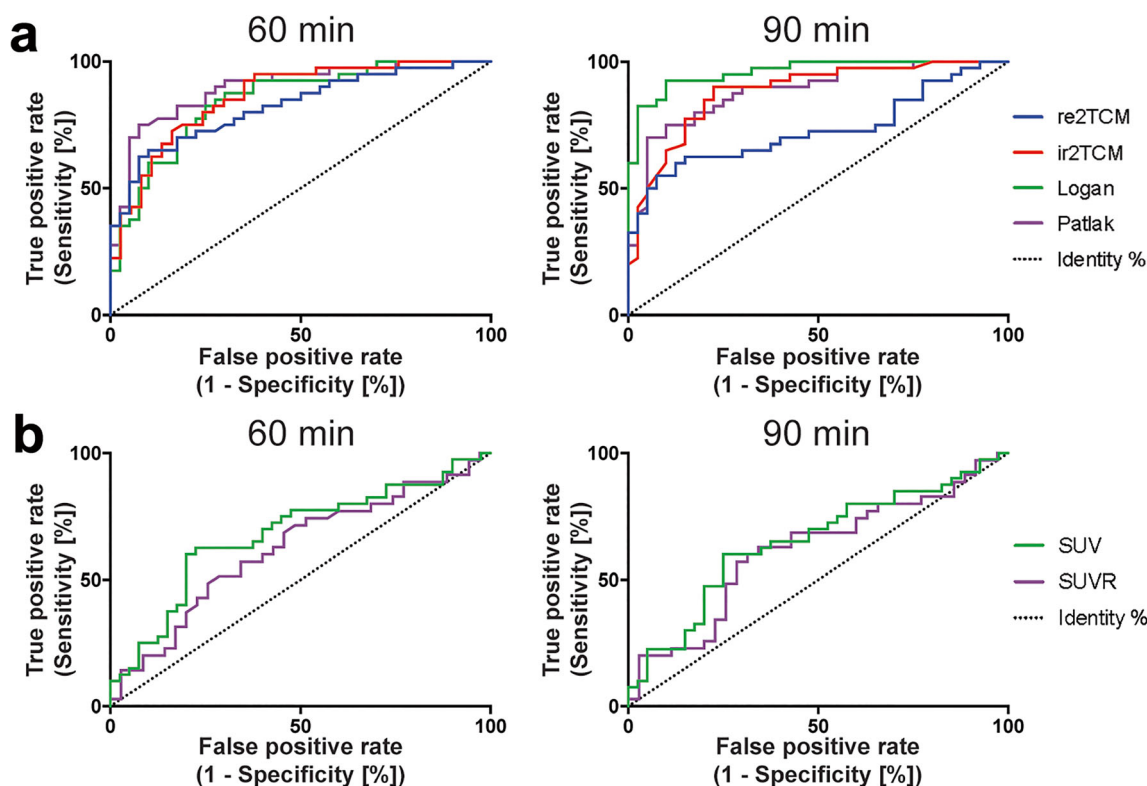
Fig. 2 Receiver operator curves of plasma input models (**a**) and the simplified measures. **b** For 60 and 90 min (re2TCM, reversible 2TCM; ir2TCM, irreversible 2TCM).

decrease in the brainstem (41 %) and smallest in the cerebellum (31 %). For 90 min, a significant decrease in K_i was found for all regions (32 ± 4 %; $p < 0.05$), with the largest decrease in the striatum (37 %) and the smallest in the cerebellum (27 %).

The AUC of the ROC analysis was highest for Logan analysis with 90 min (0.95), followed by the irreversible models (0.86–0.9) (Fig. 2). The lowest AUC was found for the reversible 2TCM (60 min, 0.83; 90 min, 0.73).

Simplified Measures

Irreversible Reference Tissue Model   Visual assessment of the model fit for RPatlak showed poor agreement for all regions except striatum (Suppl. Fig. 2, see ESM). The estimated K_i^{ref} values ranged between -0.001 and 0.011 min^{-1} for 60 min in the control group (COV 27–303 %) and -0.003–0.007 min^{-1} in the pretreatment group (COV 25–558 %). The range was similar for 90 min, with K_i^{ref} values of -0.003–0.008 min^{-1} for control and -0.004–0.004 min^{-1} for pretreated rats. Linear regression of K_i from the irreversible 2TCM and K_i^{ref} from RPatlak showed moderate R^2 for control (60 min, $R^2 = 0.49$, K_i^{ref}(Patlak) = $0.1 + 7.5 * K_i$(2TCM), $p < 0.001$; 90 min, $R^2 = 0.38$, K_i^{ref}(Patlak) = $0.1 + 7.3 * K_i$(2TCM), $p < 0.001$) and poor R^2 for pretreated rats (60 min, $R^2 = 0.10$, K_i^{ref}(Patlak) = $0.08 +$ $2.2 * K_i$(2TCM), $p = 0.07$); 90 min, $R^2 = 0.14$, K_i^{ref}(Patlak) = $0.1 + 2.9 * K_i$(2TCM), $p = 0.25$).

SUV and SUVR   SUV values at 30–60 min were 0.87–1.97 (COV 4–12 %, Table 2) for different brain regions in the control and 0.74–1.86 (COV 13–19 %) in the pretreatment group. Similar COV and SUV values were found at 50–90 min (control, 0.80 to 1.95, pretreated, 0.74 to 1.78). Linear regression with K_i from irreversible 2TCM (90 min) showed good correlations in the control group (30–60 min, $R^2 = 0.70$; 50–90 min, $R^2 = 0.82$; $p < 0.0001$). In the pretreated group, poor correlations between SUV and K_i were found ($R^2 = 0.33$–0.43, $p < 0.0001$). SUVR showed the lowest variation (COV for 30–60 and 50–90 min, 5–16 %). For 30–60 min, SUVR was 1.21–2.02 for the control group and 1.14–1.86 in the pretreatment group. SUVR of 1.19–2.17 were calculated for control and between 1.11 and 1.90 for the pretreatment group for 50–90 min. Correlation of SUVR with K_i from irreversible 2TCM (90 min) showed higher R^2 values in the control than the pretreated group (control, $R^2 = 0.66$–0.70, $p < 0.0001$; pretreated, $R^2 = 0.25$–0.26, $p = 0.002$).

Sensitivity of Simplified Measures to VAChT Saturation   The SUV and SUVR were decreased by pretreatment with FEOBV (1–18 %). The decrease was found to be statistically

Table 2. Outcome of SUV and SUVR for control and FEOBV group. Significant differences between control and pretreatment group are indicated as ***$p < 0.0005$, **$p < 0.005$, *$p < 0.05$. Shown are mean ± standard deviation ($n = 5$) for SUV, SUVR, and AIC and the range of the COV.

Brain region	SUV		SUVR	
	Control	FEOBV	Control	FEOBV
60 min				
Brainstem	1.30 ± 0.09	1.07 ± 0.13*	1.41 ± 0.05	1.24 ± 0.07**
Cerebellum	0.93 ± 0.04	0.86 ± 0.12		
Cortex	1.14 ± 0.09	1.05 ± 0.17	1.24 ± 0.06	1.23 ± 0.07
Frontal cortex	1.46 ± 0.09	1.31 ± 0.19	1.57 ± 0.11	1.53 ± 0.11
Hippocampus	1.20 ± 0.08	1.10 ± 0.19	1.29 ± 0.07	1.28 ± 0.11
Hypothalamus	1.39 ± 0.13	1.19 ± 0.17*	1.50 ± 0.08	1.38 ± 0.14*
Striatum	1.64 ± 0.2	1.46 ± 0.29	1.77 ± 0.16	1.69 ± 0.13
Thalamus	1.38 ± 0.06	1.24 ± 0.21	1.49 ± 0.05	1.44 ± 0.16
COV	4–12 %	13–19 %	5–16 %	3–8 %
90 min				
Brainstem	1.18 ± 0.09	1.00 ± 0.11*	1.39 ± 0.07	1.22 ± 0.07*
Cerebellum	0.86 ± 0.04	0.82 ± 0.11		
Cortex	1.03 ± 0.09	0.98 ± 0.14	1.22 ± 0.07	1.19 ± 0.07
Frontal cortex	1.28 ± 0.08	1.20 ± 0.17	1.53 ± 0.11	1.47 ± 0.13
Hippocampus	1.06 ± 0.08	1.00 ± 0.15	1.27 ± 0.11	1.22 ± 0.07
Hypothalamus	1.25 ± 0.1	1.10 ± 0.13	1.49 ± 0.14	1.34 ± 0.08
Striatum	1.56 ± 0.23	1.40 ± 0.27	1.78 ± 0.14	1.70 ± 0.16
Thalamus	1.20 ± 0.08	1.10 ± 0.17	1.45 ± 0.16	1.34 ± 0.08
COV	5–13 %	10–18 %	2–12 %	5–9 %

COV coefficient of variation

significant only in the brainstem (SUV, 18 %; SUVR, 12 %; $p < 0.05$) and hypothalamus (SUV, 14 %; SUVR, 8 %; $p < 0.05$) for 30–60 min, and in the brainstem for 50–90 min (SUV, 15 %; SUVR, 12 %; $p < 0.05$). The AUC of the ROC analysis (Fig. 2) was higher for SUV (30–60 min, 0.72; 50–90 min, 0.68) than for SUVR (30–60 min and 50–90 min, 0.62).

Test-Retest

The test-retest PET scans were analyzed with SUV for 30–60 and 50–90 min (Supplemental Table 1). No statistically significant differences in SUV in the brain regions assessed were found between the test and retest scan. The test-retest variability for SUV ranged between 8 ± 7 % and 12 ± 6 %, with large variations between individual rats (Table 3, Fig. 3). The ICC values of SUV were good (30–60 min, 0.75; 50–90 min, 0.79; $p < 0.0001$).

Discussion

The aim of this study was to determine the optimal quantification method for [18F]FEOBV PET in the rat brain using a plasma input function and to verify the possibility of quantification by simplified measures. The irreversible 2TCM and Patlak analysis were found to quantify [18F]FEOBV uptake in control rats best, as they showed good visual fits with lower or comparable AIC to the reversible kinetic models. Contrarily to reversible models, K_i showed a lower variation and almost no change in K_i was found when shortening the acquisition time. The partial

Table 3. Test-retest variation [%] and ICC for SUV for 30–60 and 50–90 min. Shown are mean ± standard deviation of test-retest variation ($n = 5$).

Brain region	SUV	
	30–60 min	50–90 min
Brainstem	12 ± 6	9 ± 6
Cerebellum	11 ± 8	8 ± 7
Cortex	9 ± 8	8 ± 8
Frontal cortex	9 ± 7	8 ± 9
Hippocampus	11 ± 7	8 ± 8
Hypothalamus	11 ± 4	10 ± 6
Striatum	9 ± 7	8 ± 8
Thalamus	10 ± 10	9 ± 9
ICC	0.75, $p < 0.0001$	0.78, $p < 0.0001$

ICC intraclass correlation coefficient

saturation of VAChT by pretreatment with FEOBV did not affect model selection and resulted in a statistically significant decrease in K_i in all brain regions. SUV and SUVR correlated with K_i from the irreversible 2TCM in the control group. However, poor correlations were found when VAChT was partially saturated. This was confirmed by the low sensitivity of the simplified measures to differentiate between the control and pretreated rats. Test-retest reliability in healthy rats was good for SUV with low test-retest variability and good ICC values.

In humans, the most robust estimates of VAChT were obtained with the reversible 2TCM using the same K_1/k_2 and k_4 values across brain regions within an individual subject [7]. In rats, we found large variations in V_T with the reversible 2TCM although fixing K_1/k_2 and k_4 reduced this variation somewhat (data not shown). Nevertheless, the irreversible 2TCM resulted in more reliable estimations of rate constants and low variability of K_i, without fixing rate constants. Additionally, the irreversible 2TCM showed a higher sensitivity to detect reduced VAChT availability by FEOBV pretreatment. Both Logan and Patlak graphical analysis showed good model fits. While Logan analysis showed good sensitivity to detect reduced VAChT availability at 90 min, Patlak analysis was sensitive to detect differences in VAChT availability at both 60 and 90 min with lower variation in K_i compared to V_T from Logan analysis. V_T estimated by the reversible 2TCM and Logan analysis was decreased when the acquisition was reduced from 90 to 60 min. This is consistent with human data where acquisition times of 360 min were required for reliable estimation of VAChT availability, with shorter times leading to underestimation of BP_{ND} [7]. Contrarily, the irreversible 2TCM and Patlak analysis were affected less by shortening of the scan duration, as this increased K_i by only 10 % and 1 %, respectively. Taken together, this shows that VAChT availability can be best estimated using irreversible models.

Interestingly, the dynamic range of [18F]FEOBV in the humans was much larger with approximately 25 to 1 compared to 2 to 1 in rats using plasma input models. It is possible that VAChT expression varies between species although a recent [18F]FEOBV study showed mainly
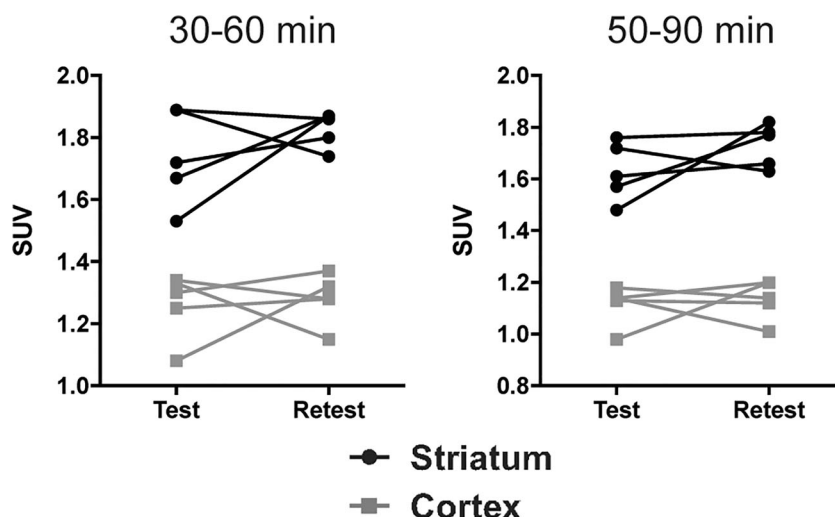
Fig. 3 Test-retest values for SUV (30–60 min, 50–90 min) for the exemplary brain regions striatum and cortex. The test value of each rat is connected to its retest value with a line.

consistent cholinergic projections in humans compared to other mammalian species [17]. It could also be related to the partial volume effect. Spill-out from the striatum could have increased the apparent binding of [^{18}F]FEOBV in surrounding regions and thus decreased the dynamic range. Future studies could apply automatic partial volume correction on rat PET data; however, this is not possible yet [18].

As kinetic modeling using a plasma input function in rats is challenging and hampers the use of [^{18}F]FEOBV PET in longitudinal experiments, we explored the use of simplified measures. Since the plasma input models indicated that irreversible models are optimal, the reference tissue Patlak model was tested. Unfortunately, while the irreversible plasma input models were found to fit the data well, the reference tissue Patlak model did not show a good fit of the data and even led to negative regression slopes. This could be explained by irreversible binding of [^{18}F]FEOBV in the reference tissue, as one of the assumptions of the reference tissue Patlak is that the reference tissue shows reversible exchange of the radiotracer between blood and tissue [19]. Indeed, we found that [^{18}F]FEOBV binding was statistically significant decreased by 36–52 % after pretreatment with FEOBV when assessed with irreversible plasma models, indicating that no suitable reference region including the cerebellum is available. The use of a pseudo-reference tissue could still be valid in animal models, *e.g.* of Parkinson's or Alzheimer's disease, in which the cholinergic neurons in the reference region are not affected. This should be carefully evaluated for each animal model and compared to results obtained from the irreversible plasma models.

Further indication of the irreversible binding of [^{18}F]FEOBV is that the uptake of [^{18}F]FEOBV remained constant between 60 and 90 min in all brain regions. This was consistent with previous studies in rats [6, 8]. The time-activity curves of [^{18}F]FEOBV in rats were similarly shaped as in humans for most brain regions, albeit with slower

kinetics [7]. An exception was the striatum, in which uptake of [^{18}F]FEOBV increased until 360 min post-injection in humans, but not in rats. This could be explained by interspecies differences in VAChT binding or expression or an effect of the isoflurane anesthesia. Indeed, isoflurane was found to suppress the release of acetylcholine [20, 21] and it has been proposed that cholinergic dysfunction after isoflurane anesthesia leads to cognitive dysfunction in older rats [22, 23]. Nevertheless, as anesthesia is necessary to perform rat PET scans it could be seen as a constant bias.

The constant uptake of [^{18}F]FEOBV at the end of the 90-min PET scan suggests the use of static imaging. In animal studies, short, static scans are preferred to minimize the effect of anesthesia on PET tracer binding and to reduce animal discomfort. The SUV at 50–90 min, mimicking static imaging, showed a good correlation with the outcome of the irreversible plasma model, but was less sensitive in detecting partial saturation of VAChT. Indeed, while most plasma input models revealed a statistically significant decrease in [^{18}F]FEOBV binding after pretreatment with FEOBV, the simplified measures were less sensitive in detecting these decreases. This was confirmed by the ROC analysis, which showed lower area-under-the-curve values for the simplified measures than the irreversible plasma models. This suggests that in future studies, if long acquisition times and arterial blood sampling are not feasible, animals might be injected with [^{18}F]FEOBV and only scanned for a short period, *e.g.*, 30 min, after an uptake period of around 60 min but that larger biological effect sizes will be necessary compared to quantification with irreversible plasma models.

In longitudinal animal studies, repeated assessment of radioligand is mostly performed without blood sampling. Thus, we determined the test-retest variability using the simplified measure SUV which showed better correlation then SUVR with K$_i$ from the irreversible 2TCM in control rats. Larger variations were found for SUV at 30–60 min

than 50–90 min resulting in slightly lower test-retest variation and higher ICC for 50–90 min SUV. This further suggests an increased stability of [18F]FEOBV SUV with longer acquisition. Nevertheless, it would be of interest to perform a test-retest study with blood sampling for quantification using irreversible plasma models as these provide the best measures of VAChT availability.

Conclusion

Our study shows that [18F]FEOBV accumulation can be reliably quantified using the irreversible 2TCM and Patlak analysis, using an acquisition time of 60 min. If blood sampling is not possible, *e.g.*, in longitudinal study designs, SUV might be used for quantification of [18F]FEOBV in rats, *e.g.*, using 50–90 min, when large biological effect sizes are expected.

Compliance with Ethical Standards.

The study protocol was approved by the Institutional Animal Care and Use Committee of the University of Groningen. All experiments were performed by licensed investigators in compliance with the Law on Animal Experiments of The Netherlands.

Conflict of Interest

The authors declare that they have no conflict of interest.

References

1. Geula C, Mesulam MM (1996) Systematic regional variations in the loss of cortical cholinergic fibers in Alzheimer's disease. Cereb Cortex 6:165–177
2. Kuhl DE, Minoshima S, Fessler JA, Frey KA, Foster NL, Ficaro EP, Wieland DM, Koeppe RA (1996) In vivo mapping of cholinergic terminals in normal aging, Alzheimer's disease, and Parkinson's disease. Ann Neurol 40:399–410
3. Whitehouse PJ, Hedreen JC, White CL, Price DL (1983) Basal forebrain neurons in the dementia of Parkinson disease. Ann Neurol 13:243–248
4. Gilmor ML, Erickson JD, Varoqui H, Hersh LB, Bennett DA, Cochran EJ, Mufson EJ, Levey AI (1999) Preservation of nucleus basalis neurons containing choline acetyltransferase and the vesicular acetylcholine transporter in the elderly with mild cognitive impairment and early Alzheimer's disease. J Comp Neurol 411:693–704
5. Mulholland GK, Wieland DM, Kilbourn MR, Frey KA, Sherman PS, Carey JE, Kuhl DE (1998) [18F]fluoroethoxy-benzovesamicol, a PET radiotracer for the vesicular acetylcholine transporter and cholinergic synapses. Synapse 30:263–274
6. Kilbourn MR, Hockley B, Lee L, Sherman P, Quesada C, Frey KA, Koeppe RA (2009) Positron emission tomography imaging of (2R,3R)-5-[18F]fluoroethoxybenzovesamicol in rat and monkey brain: a radioligand for the vesicular acetylcholine transporter. Nucl Med Biol 36:489–493
7. Petrou M, Frey KA, Kilbourn MR, Scott PJ, Raffel DM, Bohnen NI, Müller ML, Albin RL, Koeppe RA (2014) In vivo imaging of human cholinergic nerve terminals with (−)-5-18F-Fluoroethoxybenzovesamicol: biodistribution, Dosimetry, and tracer kinetic analyses. J Nucl Med 55:396–404
8. Parent M, Bedard M-AA, Aliaga A et al (2012) PET imaging of cholinergic deficits in rats using [18F]fluoroethoxybenzovesamicol ([18F]FEOBV). Neuroimage 62:555–561
9. Alves IL, Vállez García D, Parente A et al (2017) Pharmacokinetic modeling of [11C]flumazenil kinetics in the rat brain. EJNMMI Res 7:17
10. Willson JE, Brown DE, Timmens EK (1965) A toxicologic study of dimethyl sulfoxide. Toxicol Appl Pharmacol 7:104–112
11. Mulholland GK, Jung Y-W, Wieland DM et al (1993) Synthesis of [18F]Fluoroethoxy-benzovesamicol, a radiotracer for cholinergic neurons. J Label Compd Radiopharm 33:583–591
12. Vállez Garcia D, Casteels C, Schwarz AJ et al (2015) A standardized method for the construction of tracer specific PET and SPECT rat brain templates: validation and implementation of a toolbox. PLoS One 10:e0122363
13. Logan J, Fowler JS, Volkow ND, Wolf AP, Dewey SL, Schlyer DJ, MacGregor R, Hitzemann R, Bendriem B, Gatley SJ (1990) Graphical analysis of reversible radioligand binding from time-activity measurements applied to [N-11C-methyl]-(-)-cocaine PET studies in human subjects. J Cereb Blood Flow Metab 10:740–747
14. Patlak CS, Blasberg RG, Fenstermacher JD (1983) Graphical evaluation of blood-to-brain transfer constants from multiple-time uptake data. J Cereb Blood Flow Metab 3:1–7
15. Shrout PE, Fleiss JL (1979) Intraclass correlations: uses in assessing rater reliability. Psychol Bull 86:420–428
16. Zweig MH, Campbell G (1993) Receiver-operating characteristic (ROC) plots: a fundamental evaluation tool in clinical medicine. Clin Chem 39(4):561–577
17. Albin RL, Bohnen NI, Muller MLTM, Dauer WT, Sarter M, Frey KA, Koeppe RA (2018) Regional vesicular acetylcholine transporter distribution in human brain: a [18F]fluoroethoxybenzovesamicol positron emission tomography study. J Comp Neurol 526:2884–2897
18. Herfert K, Mannheim JG, Kuebler L et al (2019) Quantitative rodent brain receptor imaging. Mol Imaging Biol:1–22
19. Patlak CS, Blasberg RG (1985) Graphical evaluation of blood-to-brain transfer constants from multiple-time uptake data. Generalizations J Cereb Blood Flow Metab 5:584–590
20. Shichino T, Murakawa M, Adachi T, Nakao S, Shinomura T, Kurata J, Mori K (1997) Effects of isoflurane on in vivo release of acetylcholine in the rat cerebral cortex and striatum. Acta Anaesthesiol Scand 41:1335–1340
21. Whittington RA, Virág L (2010) The differential effects of equipotent doses of isoflurane and desflurane on hippocampal acetylcholine levels in young and aged rats. Neurosci Lett 471:166–170
22. Su D, Zhao Y, Wang B et al (2011) Isoflurane-induced spatial memory impairment in mice is prevented by the acetylcholinesterase inhibitor donepezil. PLoS One 6:e27632
23. Ni C, Tan G, Luo A, Qian M, Tang Y, Zhou Y, Wang J, Li M, Zhang Y, Jia D, Wu C, Guo X (2013) Melatonin premedication attenuates isoflurane anesthesia-induced β-amyloid generation and cholinergic dysfunction in the hippocampus of aged rats. Int J Neurosci 123:213–220

Publisher's Note Springer Nature remains neutral with regard to jurisdictional claims in published maps and institutional affiliations.